Computational Identification of Transition-Metal Dichalcogenides for Electrochemical CO_2 Reduction to Highly Reduced Species Beyond CO and HCOOH

Sungwoo Kang, [†] *Suyeon Ju,*[†] *Seungwu Han*[†] *and Youngho Kang*[‡,*]

[†]Department of Materials Science and Engineering, Seoul National University, Seoul 08826, Korea.

[‡]Department of Materials Science and Engineering, Incheon National University, Incheon 22012, Korea.

*Corresponding author: youngho84@inu.ac.kr

Derivation of the equation 1 in the main text

The free energy of intermediate $*C_xH_yO_z$ is written as follows:

$$G^U\left(*C_xH_yO_z{}^q\right) = E\left(*C_xH_yO_z{}^q\right) - E(*) - x\mu(\mathrm{C}) - y\mu(\mathrm{H}) - z\mu(\mathrm{O}) + q\mu(\mathrm{e}) + E_{\mathrm{add}}, \quad (S1)$$

where μ(C), μ(H), μ(O), and μ(e) are the chemical potential of C, H, O, and electron. These are expressed as follows:[S1]

$$\mu(\mathrm{H}) = \frac{1}{2}G(\mathrm{H_2}) - eU, \quad (S2)$$

$$\mu(\mathrm{O}) = G(\mathrm{H_2O}) - 2\mu(\mathrm{H}), \quad (S3)$$

$$\mu(\mathrm{C}) = G(\mathrm{CO_2}) - 2\mu(\mathrm{O}). \quad (S4)$$

Using equations S1-S4, we get

$$G\left(*C_xH_yO_z{}^q\right) = E\left(*C_xH_yO_z{}^q\right) - E(*) - xG(\mathrm{CO_2}) - 0.5(4x + y - 2z)G(\mathrm{H_2}) - (z - 2x)G(\mathrm{H_2O}) + (4x + y - 2z)eU + q\mu(\mathrm{e}) + E_{\mathrm{add}}. \quad (S5)$$

Then, μ(e) can be calculated as follows:[S2]

$$q\mu(\mathrm{e}) = q\mu_{\mathrm{SHE}}(\mathrm{e}) + 0.059\mathrm{pH} - eU, \quad (S6)$$

Using equations S5 and S6, we get the final equation in the main text:

$$G^U\left(*C_xH_yO_z{}^q\right) = E\left(*C_xH_yO_z{}^q\right) - E(*) - xG(\mathrm{CO_2}) - 0.5(4x + y - 2z)G(\mathrm{H_2}) - (z - 2x)G(\mathrm{H_2O}) + (4x + y - 2z)eU - eqU + 0.059\mathrm{pH} \times q + q\mu_{\mathrm{SHE}}(e^-) + E_{\mathrm{add}}. \quad (S7)$$

Details of the charge state calculations

We present all neutral free energies ($G^0\left(*C_xH_yO_z{}^0\right)$) in Table S1 and charging energies ($G^0\left(*C_xH_yO_z{}^q\right) - G^0\left(*C_xH_yO_z{}^0\right)$) in Table S2. The free energies of neutral species can be easily calculated from Table S1 using theoretical framework of previous work.[S1] The free energies of charged adsorbates can be calculated using equation S7. Here, one can obtain free energies of charged adsorbate using Table S1 and S2 as follows

$$G^U\left(*C_xH_yO_z{}^q\right) = G^0\left(*C_xH_yO_z{}^0\right) + \left[G^0\left(*C_xH_yO_z{}^q\right) - G^0\left(*C_xH_yO_z{}^0\right)\right] - (4x + y - 2z - q)eU, \quad (S6)$$

where the first energy term is written in Table S1, and the second energy term is written in Table S2. Among the possible charge states, we choose the most energetically favorable one.

Note that these energies are differently dependent with charges for different types of intermediates. Therefore, relative energies between intermediates can change with respect to the U even it is in the same protonation step (e.g. *COOH and *OCHO). For instance, in the case of MoS_2 in Figure S2a, energy difference between *COOH and *OCHO increases when U changes from 0 to −1 V. Due to this charge dependence, maximum potential steps of PtS_2, $PtSe_2$, $PtTe_2$, $IrTe_2$, and SnS_2 are not reduced to 0 eV as presented in Figure S2. Note that we omit ReS_2 and $ReSe_2$ in Figure S2 because charge states of all their intermediates remain 0 from 0 to −1 V.

Geometries of *COOH, *O and *OH

We choose the most stable atomic configurations for vacancy sites of TMDs. For *COOH, we tested three configurations shown in Figure S3 for several TMDs, and atomic configuration in Figure S3a is found to be the most stable among these. For *O, *OH, and *OCHO, we find that atomic configurations in Figure S4 are the most favorable. Note that atomic configurations of *COOH and *OH is in good agreement with the atomic geometries presented in ref. S3.

Table S1. Free energies of uncharged adsorbates. The energy unit is eV.

	G^0(*H^0)	G^0(*OCHO^0)	G^0(*COOH^0)	G^0(*O^0)	G^0(*OH^0)
TiS2	0.43	-0.13	0.79	-0.23	-0.50
TiSe2	0.16	-0.46	0.41	-0.85	-0.79
TiTe2	-0.24	-0.90	0.08	-1.70	-1.19
ZrS2	0.46	-0.11	0.85	-0.81	-0.40
ZrSe2	0.54	-0.41	0.49	-1.12	-0.63
ZrTe2	0.12	-0.81	-0.15	-1.63	-0.92
HfS2	-0.24	-1.28	-0.43	-2.22	-1.70
HfSe2	-0.37	-1.40	-0.66	-2.31	-1.74
HfTe2	-0.33	-1.48	-0.90	-2.26	-1.57
VS2	0.07	-0.37	0.53	-0.16	-0.89
VSe2	-0.14	-0.34	0.51	-0.44	-0.68
VTe2	-0.57	-0.61	0.58	-1.36	-1.14
NbS2	0.16	-0.47	0.18	-0.03	-0.90
NbSe2	-0.15	-0.74	-0.16	-0.59	-1.04
NbTe2	0.23	-0.17	0.18	-0.41	-0.42
TaS2	0.00	-0.83	-0.30	-0.65	-1.26
TaSe2	-0.43	-1.11	-0.70	-1.30	-1.46
TaTe2	-0.15	-0.81	-0.73	-1.17	-1.04
CrSe2	0.01	-0.31	0.41	0.19	-0.52
CrTe2	-0.34	-0.76	-0.20	-0.52	-0.93
MoS2	-0.14	0.18	0.87	-1.04	-0.22
MoSe2	-0.37	-0.05	0.64	-1.03	-0.28
MoTe2	-0.47	-0.30	0.23	-1.07	-0.46
WS2	-0.10	0.19	0.80	-1.29	-0.04
WSe2	-0.18	0.09	0.63	-1.37	-0.04
WTe2	-0.80	-0.63	-0.54	-0.06	-0.49
ReS2	0.14	0.30	1.11	-0.06	0.04
ReSe2	-0.07	0.02	0.53	0.09	0.05
ReTe2	-0.33	-0.21	-0.33	0.58	0.06
CoTe2	-0.14	-0.13	0.51	2.18	0.95
IrTe2	-0.59	0.11	-0.36	1.70	0.63
NiTe2	0.33	0.57	0.70	2.53	1.27
PdTe2	0.31	0.54	0.80	2.73	1.27
PtS2	-0.04	0.52	0.17	1.28	0.63

PtSe2	-0.17	0.33	-0.01	1.53	0.66
PtTe2	-0.22	0.25	0.02	2.18	0.97
SnS2	-0.02	-0.44	0.14	-0.22	-0.68
SnSe2	0.47	-0.07	0.47	0.70	-0.05

Table S2. Charging energy at 0 V vs. RHE [$G^0(*C_xH_yO_z^q) - G^0(*C_xH_yO_z^0)$] of adsorbates are presented for possible charge states. N/C in *H column indicates "Not calculated" in the case when the free energy steps of intermediates does not reduced to 0 (see section 2 for details).

	V_X		*OCHO		*O		*OH		*COOH		*H	
	q	Energy	q	Energy	q	Energy	q	Energy	q	Energy	q	Energy
MoS2	-4	0.40										
	-3	-0.06	-3	0.69			-3	1.24	-3	1.27	-3	0.24
	-2	-0.37	-2	0.12			-2	0.69	-2	0.56	-2	-0.34
	-1	-0.42	-1	-0.17			-1	-0.68	-1	-0.06	-1	-0.52
	0	0.00	0	0.00	0	0.00	0	0.00	0	0.00	0	0.00
	1	1.65	1	0.59			1	0.31	1	0.42	1	1.09
	2	4.96										
MoSe2	-4	2.54										
	-3	1.22	-3	1.71			-3	2.26	-3	2.30	-3	1.33
	-2	0.26	-2	0.91			-2	1.24	-2	1.15	-2	0.39
	-1	-0.07	-1	0.27			-1	0.57	-1	0.22	-1	-0.11
	0	0.00	0	0.00	0	0.00	0	0.00	0	0.00	0	0.00
	1	1.29	1	0.08			1	-0.09	1	-0.07	1	0.62
	2	2.90		1.71								
MoTe2	-4	2.84										
	-3	1.59	-3	1.81			-3	2.16	-3	2.34	-3	1.79
	-2	0.60	-2	1.04			-2	1.24	-2	1.08	-2	0.78
	-1	0.13	-1	0.45			-1	0.60	-1	0.46	-1	0.13
	0	0.00	0	0.00	0	0.00	0	0.00	0	0.00	0	0.00
	1	0.79	1	-0.09			1	-0.20	1	-0.29	1	0.29
	2	1.86										
WS2	-4	2.57										
	-3	1.25	-3	1.30			-3	2.00	-3	1.94	-3	1.21
	-2	0.38	-2	0.59			-2	0.99	-2	0.83	-2	0.22
	-1	-0.11	-1	0.08			-1	0.36	-1	-0.11	-1	-0.20
	0	0.00	0	0.00	0	0.00	0	0.00	0	0.00	0	0.00

	1	1.62	1	0.10			1	-0.16	1	0.10	1	0.75
	2	3.60		1.30								
WSe2	-4	3.57										
	-3	2.35	-3	2.06			-3	2.56	-3	2.51	-3	2.24
	-2	1.08	-2	1.09			-2	1.32	-2	1.32	-2	0.96
	-1	0.24	-1	0.36			-1	0.44	-1	0.18	-1	0.22
	0	0.00	0	0.00	0	0.00	0	0.00	0	0.00	0	0.00
	1	1.15	1	-0.20			1	-0.48	1	-0.27	1	0.33
	2	2.66										
IrTe2	-4	-0.19										
	-3	-0.30										
	-2	-0.41										
	-1	-0.31	-1	-0.18			-1	0.06	-1	-0.18		
	0	0.00	0	0.00	0	0.00	0	0.00	0	0.00	N/C	N/C
	1	0.61	1	0.58			1	0.39	1	0.59		
	2	1.31										
PtS2	-4	-1.44										
	-3	-1.42										
	-2	-1.23										
	-1	-0.73	-1	-0.78			-1	-0.45	-1	-0.80		
	0	0.00	0	0.00	0	0.00	0	0.00	0	0.00	N/C	N/C
	1	1.70	1	1.21			1	0.89	1	1.36		
	2	3.71										
PtSe2	-4	-0.31										
	-3	-0.54										
	-2	-0.60										
	-1	-0.42	-1	-0.47			-1	-0.27	-1	1.99		
	0	0.00	0	0.00	0	0.00	0	0.00	0	0.00	N/C	N/C
	1	1.14	1	0.93			1	0.80	1	-1.58		
	2	2.57										
PtTe2	-4	0.86										
	-3	0.39										
	-2	0.06										
	-1	-0.07	-1	-0.11			-1	0.09	-1	0.09		
	0	0.00	0	0.00	0	0.00	0	0.00	0	0.00	N/C	N/C
	1	0.49	1	0.51			1	0.26	1	0.35		
	2	1.19										
ReS2	0	0.00	0	0.00	0	0.00	0	0.00	0	0.00	0	0.00

	1	1.46	1	0.52					1	0.31	1	0.60
	2	3.12										
ReSe2	0	0.00	0	0.00	0	0.00	0	0.00	0	0.00	0	0.00
	1	0.91	1	0.32			1	0.06	1	-0.09	1	0.27
	2	2.07										
ReTe2											-3	1.61
	-2	1.09									-2	0.74
	-1	0.39	-1	0.40					-1	0.48	-1	0.15
	0	-0.01	0	0.00	0	0.00	0	0.00	0	0.00	0	0.00
	1	-0.36	1	0.18					1	-0.25	1	0.18
	2	0.99										
SnS2	-2	-2.15										
	-1	-1.13										
	0	0.02	0	0.00	0	0.00	0	0.00	0	0.00	N/C	N/C
	1	-1.03										
	2	2.07										

Table S3. E_{add} values of intermediates.

	*OCHO	*COOH	*O	*OH	*H
E_{add} (eV)	0.57	0.60	0.14	0.37	0.16

Table S4. Details of TMDs.

TMD	Structure	Metal (M) / Semiconductor (SM)	E_f (eV)
TiS2	T	M	0.71
TiSe2	T	M	1.67
TiTe2	T	M	2.60
ZrS2	T	SM w/o midgap states	1.12
ZrSe2	T	SM w/o midgap states	1.73
ZrTe2	T	M	2.37
HfS2	T	SM w/o midgap states	2.53
HfSe2	T	SM w/o midgap states	2.97
HfTe2	T	M	3.04
VS2	H	M	1.19

VSe2	T	M	1.59
VTe2	T	M	2.02
NbS2	H	M	1.16
NbSe2	H	M	1.93
NbTe2	H	M	1.80
TaS2	H	M	1.56
TaSe2	H	M	2.41
TaTe2	H	M	2.69
CrSe2	T	M	1.35
CrTe2	T	M	2.30
MoS2	H	SM	2.36
MoSe2	H	SM	2.89
MoTe2	H	SM	3.38
WS2	H	SM	2.67
WSe2	H	SM	2.96
WTe2	T′	M	3.09
ReS2	T″	SM	1.94
ReSe2	T″	SM	2.59
ReTe2	T″	SM	3.30
CoTe2	T′	M	1.84
IrTe2	T″	SM	3.02
NiTe2	T	M	1.46
PdTe2	T	SM w/o midgap states	1.89
PtS2	T	SM	1.55
PtSe2	T	SM	2.23
PtTe2	T	SM	2.67
SnS2	T	SM	2.53
SnSe2	T	SM w/o midgap states	2.20

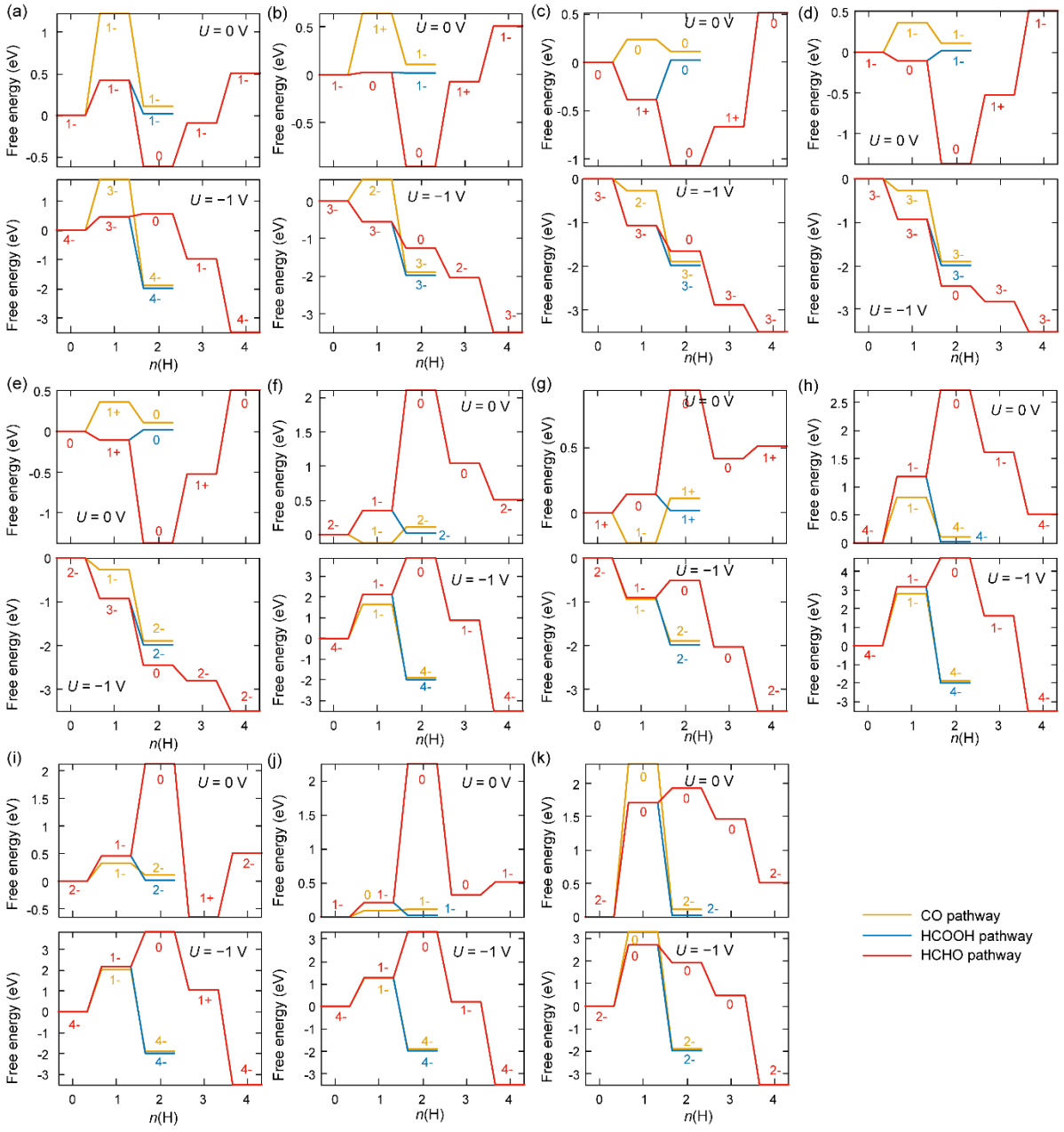

Figure S1. Free energies of all pathways at 0 V and -1 V of (a) MoS_2, (b) $MoSe_2$, (c) $MoTe_2$, (d) WS_2, (e) WSe_2, (f) $IrTe_2$, (g) $ReTe_2$, (h) PtS_2, (i) $PtSe_2$, (j) $PtTe_2$, and (k) SnS_2.

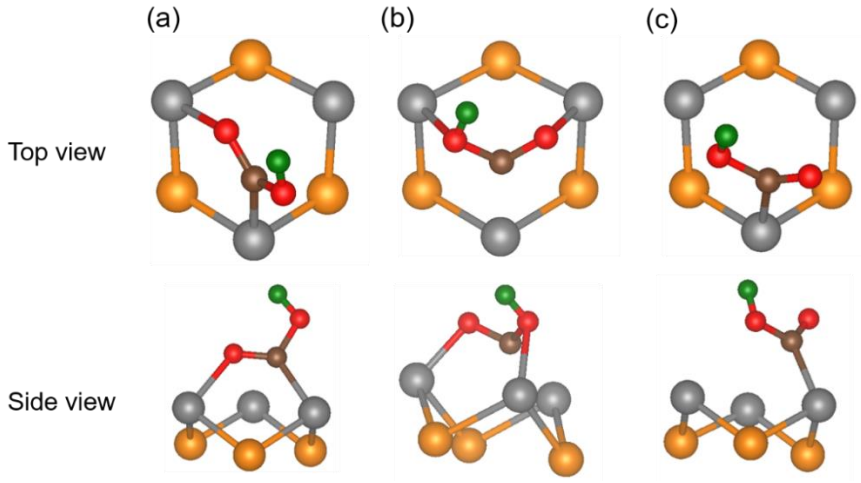

Figure S2. Atomic configurations of *COOH considered in this study. Gray atoms are transition metals, orange atoms are chalcogen atoms, black atoms are C, red atoms are O, and green atoms are H.

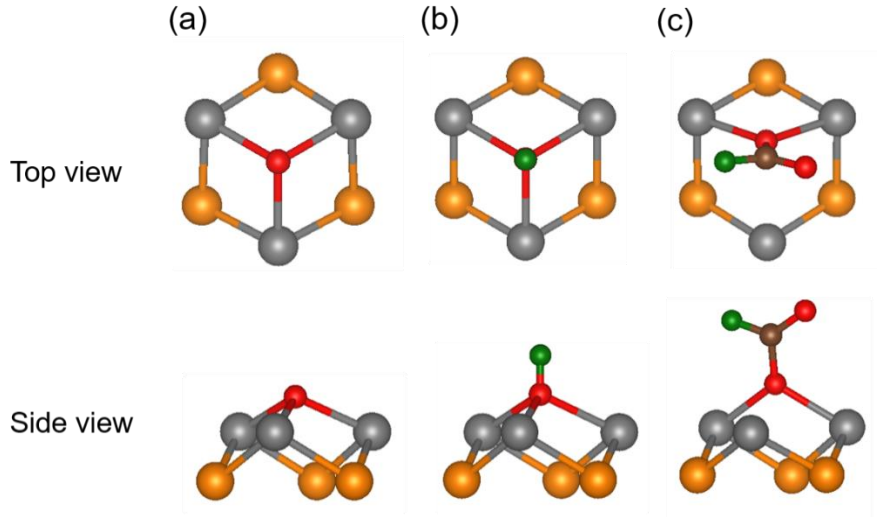

Figure S3. Adsorption configurations of (a) *O, (b) *OH, and (c) *OCHO considered in this study.

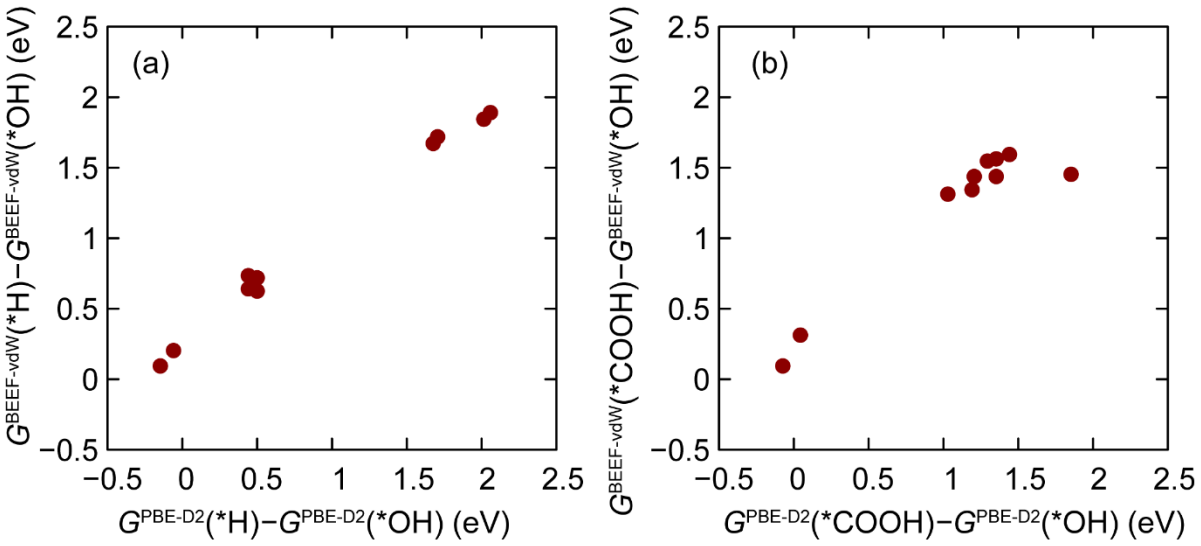

Figure S4. The comparison of calculation results between PBE-D2 functional and BEEF-vdW functional for (a) G^0(*H)-G^0(*OH), and (b) G^0(*COOH)-G^0(*OH). BEEF-vdW functional is known to be accurate in describing chemisorption energies of atoms or molecules on solid surfaces. The BEEF-vdW results are adopted from ref. 15.

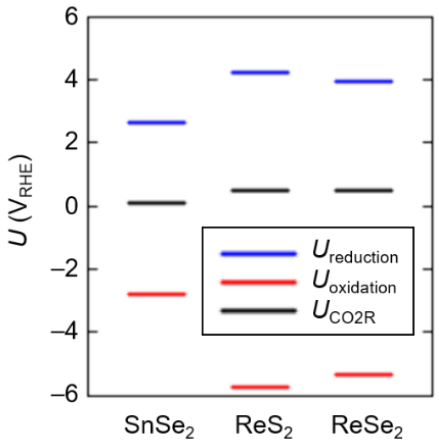

Figure S5. Calculated oxidation and reduction leaching potential and potential for CO_2R of $SnSe_2$, ReS_2, and $ReSe_2$.

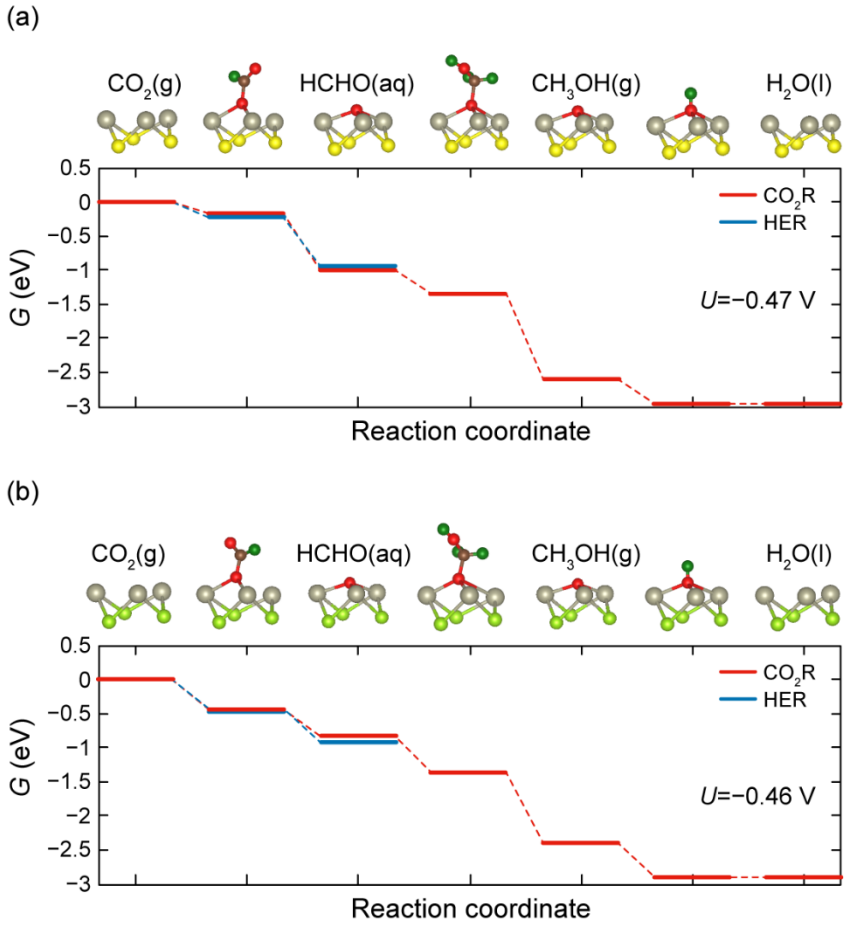

Figure S6. The free-energy diagrams for the pathway to CH_3OH of (a) ReS_2 and (b) $ReSe_2$.

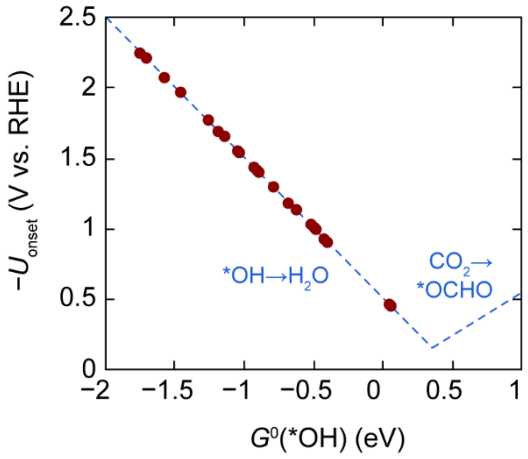

Figure S7. Volcano plot of $-U_{onset}$ as a function of G^0(*OH).

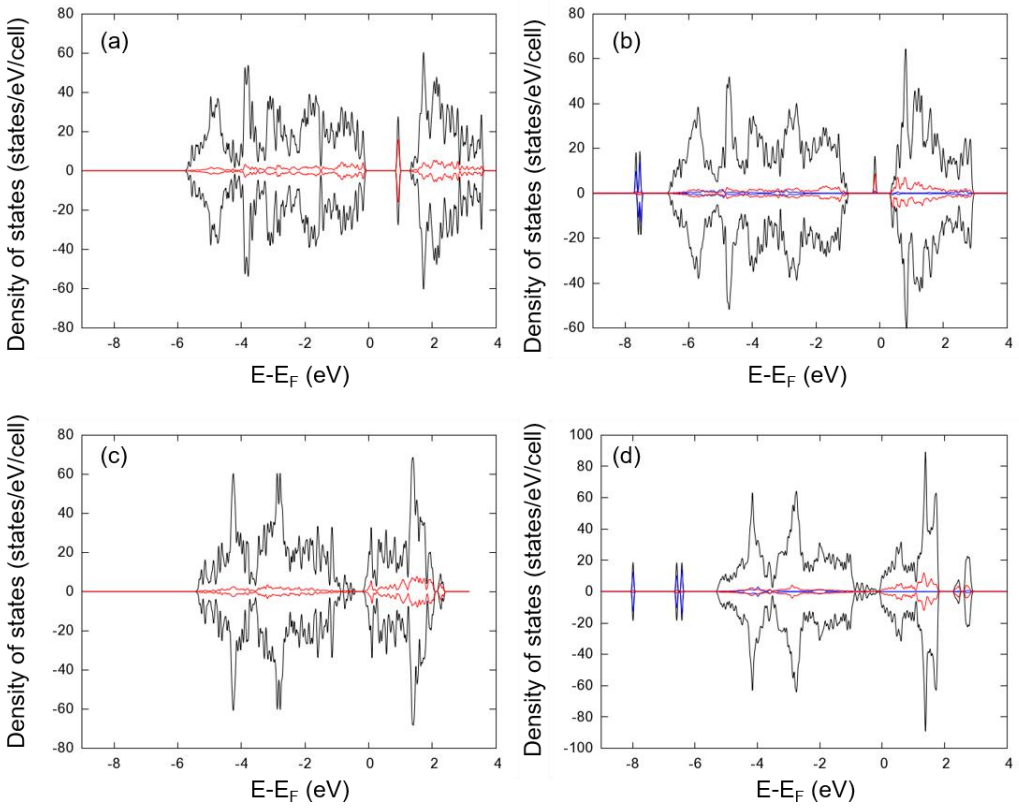

Figure S8. Density of states (DOS) of (a) V_{Se}-$MoSe_2$, (b) *OCHO-$MoSe_2$, (c) V_S-TiS_2, and (d)

*OCHO-TiS_2. Black, red, and blue lines are total DOS, projected DOS of near-vacancy atoms, and adsorbate, respectively.

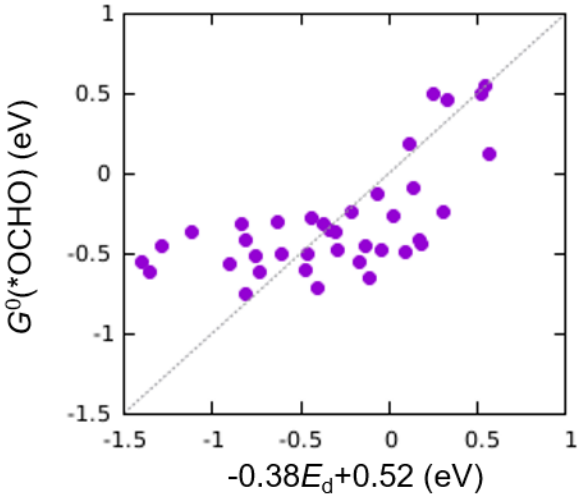

Figure S9. Regression result showing the correlation between G^0(*OCHO) and d-band center (E_d).

REFERENCES

(S1) Peterson, A. A.; Abild-Pedersen, F.; Studt, F.; Rossmeisl, J.; Nørskov, J. K. How Copper Catalyzes the Electroreduction of Carbon Dioxide into Hydrocarbon Fuels. *Energy Environ. Sci.* **2010**, *3* (9), 1311–1315.

(S2) Nørskov, J. K.; Rossmeisl, J.; Logadottir, A.; Lindqvist, L.; Kitchin, J. R.; Bligaard, T.; Jónsson, H. Origin of the Overpotential for Oxygen Reduction at a Fuel-Cell Cathode. *J. Phys. Chem. B* **2004**, *108* (46), 17886–17892.

(S3) Ji, Y.; Nørskov, J. K.; Chan, K. Scaling Relations on Basal Plane Vacancies of Transition Metal Dichalcogenides for CO_2 Reduction. *J. Phys. Chem. C* **2019**, *123* (7), 4256–4261.